

Cite this: *Soft Matter*, 2012, **8**, 667

www.rsc.org/softmatter

PAPER

Non-equilibrium cluster states in colloids with competing interactions

Tian Hui Zhang,^{*a} Jan Klok,^b R. Hans Tromp,^b Jan Groenewold^a and Willem K. Kegel^{*a}

Received 17th August 2011, Accepted 10th October 2011

DOI: 10.1039/c1sm06570j

Cluster formation and gelation are studied in a colloidal model system with competing short-range attractions and long-range repulsions. In contrast to predictions by equilibrium theory, the size of clusters spontaneously formed at low colloidal volume fractions decreases with increasing strength of the short-range attraction. Moreover, the microstructure and shape of the clusters sensitively depend on the strength of the short-range attraction: from compact and crystalline clusters at relatively weak attractions to disordered and quasi-linear clusters at strong attractions. By systematically varying attraction strength and colloidal volume fraction, we observe gelation at relatively high volume fraction. The structure of the gel depends on attraction strength: in systems with the lowest attraction strength, crowding of crystalline clusters leads to microcrystalline gels. In contrast, in systems with relatively strong attraction strength, percolation of quasi-linear clusters leads to low-density gels. In analyzing the results we show that nucleation and rearrangement processes play a key role in determining the properties of clusters and the mechanism of gelation. This study implies that by tuning the strength of short-range attractions, the growth mechanism as well as the structure of clusters can be controlled, and thereby the route to a gel state.

Introduction

Colloidal particles with short-range attractions between them form analogs of the molecular aggregation states, solid, liquid, and gas,¹ as well as non-equilibrium states such as a glass and a gel state.^{2,3} Recently, it was found that if the attractive forces are supplemented with a relatively long-range repulsion, a cluster phase is stable at low volume fractions. Computer simulations suggest that the shape of the clusters ranges from spherical to linear and that the spherical shape is marginally stable.^{4,5} The common understanding of cluster phases is that because of the competition between the short-range attractions and the long-range repulsions, clusters with a finite equilibrium size N_{eq} are stable with respect to dense bulk phases.^{6–8} The equilibrium size N_{eq} is predicted to increase with the colloidal volume fraction ϕ_c and the strength of short-range interactions U by $N_{\text{eq}} \propto -U\phi_c$,⁶ which, at least at constant U , has indeed been verified experimentally.^{7,9} At high volume fractions both simulations and experiments indicate that colloids form a gel state. Percolation, characterized by elongation and branching of clusters, was suggested to be responsible for the dynamic arrest into a gel.^{7,10–13} Next to percolation, mechanisms including jamming¹⁴ and glass transition of clusters¹⁵ have been suggested to explain the formation of gels. However, no consensus has been reached so far. Here we systematically study the effect of the strength of

short-range attractions U on microphase separations and gelation. We find that in contrast to the prediction of equilibrium theory, the clusters formed at low volume fractions become smaller upon increasing U . Moreover, in the subsequent growth driven by the increase of local colloidal volume fractions, clusters in solutions with different attraction strengths exhibit distinct morphologies: the stronger the attractions, the more elongated the structures are. These observations also are not in agreement with predictions based on equilibrium clusters.^{5,6} This study points to the importance of non-equilibrium effects, not only in the gel state but also in cluster phases. It also provides a means to control gel morphology by tuning the strength of the short-range attractions.

Experimental section

The colloidal particles used in this study are polymethylmethacrylate (PMMA) spheres with a mean radius of $r_c = 446$ nm and a relative polydispersity of 3%.¹⁶ The mass density is 1.17 g cm^{-3} . They are fluorescently labelled with 4-methylaminoethylmethacrylate-7-nitrobenzo-2-oxa-1,3-diazole (NBD-MAEM) and sterically stabilized against flocculation by poly(12-hydroxystearic acid). The particles are dispersed in a mixture of cyclohexyl bromide (CHB) and *cis*-decalin. In this mixture the PMMA spheres acquire a small positive charge which leads to a long-range repulsion between the particles. By adding non-adsorbing polymer (polystyrene), a short-range depletion attraction between colloidal particles is induced. The non-adsorbing polymer used in this study has a molecular weight

^aVan't Hoff Laboratory for Physical and Colloid Chemistry, Debye Research Institute, Utrecht University, Padualaan 8, 3584 CH Utrecht, The Netherlands. E-mail: w.k.kegel@uu.nl; tianhui.zhang@hotmail.com

^bNIZO Food Research, Kernhemseweg 2, 6718 ZB Ede, The Netherlands

of 200 000 g mol⁻¹ and a mean radius of gyration $r_g = 12.5$ nm. The minimum of the short-range attractive potential U is determined by the polymer volume fraction ϕ_p using $U/k_B T = -0.5\phi_p(2 + 3/\xi)$, where $\xi = r_g/r_c$ and ϕ_p is the fraction of the free volume of solution occupied by polymer coils.^{17,18} The range of the depletion attraction is determined by the value of r_g .

In our studies, the cluster phases are formed from equilibrium dilute phases by slow sedimentation which leads to successively higher local volume fractions. To achieve this, a small mass density difference between the colloidal particles and the solvent is applied, leading to a slow sedimentation of the colloidal particles. The Debye screening length is estimated to be $\kappa^{-1} \approx 1.6$ μm .¹⁹ All solutions are prepared in 800 μl quantities and an overall initial colloidal volume fraction $\phi_c \approx 0.006$. The local volume fraction at a certain height z in the sedimentation profile is estimated from the areal number density. The zeta potential of the particles measured using a Malvern zeta sizer is $\Psi \approx +10$ mV. This value corresponds to a net charge per particle of $Z \approx 25$ unit charges, where we used the Debye-Hückel approximation: $Z = r_c(1 + \kappa r_c)\Psi/l_B$, with $l_B = e^2/4\pi\epsilon_0\epsilon_r k_B T$ the Bjerrum length being approximately 9 nm in our system. Three-dimensional laser scanning confocal microscopy is used to resolve the structure of the gels. Observations were conducted in the region 20–40 μm away from the wall of the glass containers. The three dimensional structure analysis was carried out as follows: stacks consisting of 200 images were acquired with a resolution of 0.1 μm per pixel in the x - y plane and a plane-to-plane distance of 0.1 μm in the z direction. The stacks were analyzed with IDL routines,²⁰ and the particle positions were located with an accuracy of ~ 10 nm in the x - y plane and ~ 100 nm in the z direction. In this study, samples with different polymer volume fraction ϕ_p were prepared and the corresponding attraction potential minimum ranges roughly from $-5 k_B T$ to $-20 k_B T$. Before sedimentation samples were homogenized by shaking.

Results

The growth and structural evolution of clusters was investigated as a function of the attraction strength U and monitored in time starting from the first appearance of clusters in the slowly sedimenting systems. The results are depicted in Fig. 1. In systems with $U = -5.5 k_B T$, at a local volume fraction of 0.06, crystalline clusters with a typical size of ~ 100 colloids are observed (Fig. 1a), as in our previous studies.²¹ In order to systematically explore the effect of attraction on the properties of the clusters, observations are conducted at a similar volume fraction of 0.06 in solutions with increasing attraction strength, as set by the polymer volume fraction. In dispersions with $U = -8.8 k_B T$ (Fig. 1d) and $U = -16.5 k_B T$ (Fig. 1g), the typical sizes of clusters are measured to be ~ 10 and ~ 4 colloids, respectively. Due to the small size, it is difficult to specify their structure. However, the trend that the size of the clusters decreases with increasing the short range attraction strength is clear in Fig. 1a, d and g. This is the opposite trend as predicted by a theory that assumes fully equilibrated structures.⁶ Moreover, upon increasing the colloidal volume fractions, the shape and structure of clusters in systems with different attraction strengths evolve in different ways. In solutions with $U = -5.5 k_B T$, the crystalline clusters exhibit no

significant change upon increasing the volume fraction, both in shape and in structure (Fig. 1b). To quantify the growth of clusters upon increasing the volume fraction, the radius of gyration R_g for clusters, as a function of size N , is investigated. Because of statistics we have not resolved the local volume fractions for the measured R_g and we effectively ignore the dependence of R_g on volume fraction. In fact computer simulations have suggested that R_g indeed does not depend on volume fraction.⁵ In Fig. 1c, the fractal dimension d_f , which is defined by $\log N/\log R_g$, of the crystalline clusters is about 2.29. At the same time, the d_f defined by the largest R_g and the d_f defined by the smallest R_g are 2.30 and 2.21, respectively, which points to a narrow shape distribution of the clusters. This rather constant d_f of clusters implies that during the growth, the shape and the structure of clusters are size-independent. However, a different scenario is observed in solutions with stronger attractions. In solutions with $U = -8.8 k_B T$, Fig. 1e suggests that the clusters become elongated as their size increases. The behaviour of R_g (Fig. 1f) shows that when clusters are larger than $N \approx 20$, the range of R_g as a function of N gradually becomes broader. This broadening probably reflects the broad range in observed shapes of the clusters: from elongated, quasi-linear, to branching shapes as indicated in Fig. 1f. It follows that clusters are growing through two distinct routes: elongation and branching. These two different growth routes give rise to distinct configurations and thus different R_g . In experiments, most clusters are getting elongated as well as branching during the growth. The same growth scenario is observed in systems with $U = -16.5 k_B T$ as we can see in Fig. 1h and i but the branches in Fig. 1h seem to become thinner compared to Fig. 1e.

Discussion

First of all we address the fact that the clusters observed at $\phi_c \approx 0.06$ become smaller upon increasing the attraction strength. This observation is inconsistent with equilibrium theory⁶ which predicts that the size of equilibrium clusters increases with the attraction strength at constant colloidal volume fraction. Here, we emphasize that the decreasing cluster size cannot be explained by extending equilibrium theory with electrostatic interactions between the clusters. In fact, the only systematic variation is the attractive interaction strength, and the influence of electrostatics is constant at comparable volume fractions. In this study, we seek an explanation in terms of energy barriers and critical cluster size as a function of attraction strength. For that we take classical nucleation theory (CNT) as a guide and employ small modifications to account for the finite-size of the clusters (that is, on top of the capillary approximation) and on the long-range nature of the electrostatic interactions. We write the change in free energy $\Delta G(N)$ upon formation of a dense cluster with size N as:

$$\Delta G(N) = N\Delta\mu + \gamma A_c + G_c \quad (1)$$

where $\Delta\mu$ is the chemical potential difference between the dilute phase and the dense phase, γ is the interfacial tension and A_c is the surface area of a dense cluster. G_c is the electrostatic self-energy of the cluster. In writing down eqn (1), we have separated the attractive contributions in the first two terms from the

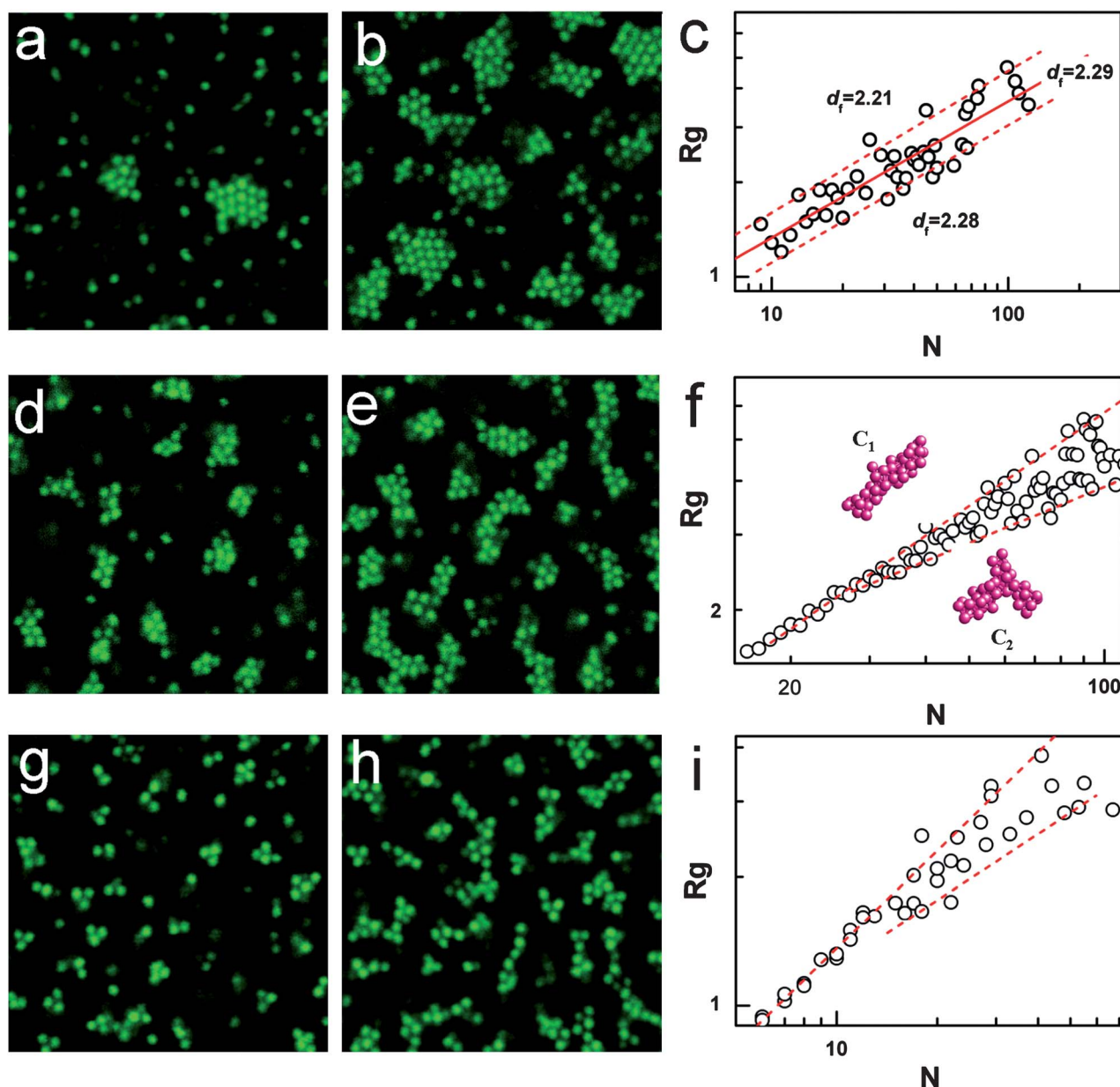


Fig. 1 (a) In solutions with $U = -5.5 k_B T$, crystalline clusters are formed at $\phi_c \approx 0.06$. (b) Upon increasing the local volume fraction to $\phi_c \approx 0.12$, more crystalline clusters are obtained. (c) The radius of gyration R_g versus cluster size N . (d) In solutions with $U = -8.8 k_B T$, relatively smaller clusters are obtained at $\phi_c \approx 0.06$. (e) As (d), but $\phi_c \approx 0.13$, clusters become larger and elongated. (f) R_g versus N for the system in (d) and (e), both linear growth and branching occur. (g) In solutions with $U = -16.5 k_B T$ and $\phi_c \approx 0.06$, clusters are smaller upon increasing the attraction strength. (h) As (g), but now $\phi_c \approx 0.10$. (i) R_g versus N for the system in (g) and (h). Every data point for $R_g \approx N$ is an average over clusters with the same size and a similar R_g .

repulsive ones in the last term. In the following, we assume the cluster has a close-packed structure (face centered cubic or hexagonally close-packed). Given the pair attraction energy U , as a first approach we take the capillary approximation and write the surface term in eqn (1) as $\gamma A_c \approx 3|U|N^{2/3}$, where we assume that each colloid at the surface misses 3 bonds. Within CNT, $\Delta\mu = -k_B T \ln S$, where S is the supersaturation given by $S = \phi_c / \phi_{\text{coex}}$. Here, ϕ_c is the colloidal volume fraction in metastable dilute phases and ϕ_{coex} is the volume fraction of the single colloids (not part of a cluster) that coexist with the clusters—in fact the ‘critical aggregation concentration’ or ‘solubility’. In general, inspired by micelle and solution theory,^{22,23}

$\phi_{\text{coex}} \approx v_c \exp(6U/k_B T) / \delta^3$. Here, v_c is the volume of a colloidal particle and δ is the interaction range, being comparable to the size of the polymer (depletant). Here we adopt $\delta = 10$ nm. The electrostatic repulsive energy G_c in eqn (1) is given by $G_c = 0.5 l_B \rho_c^2 v_c^2 N^{5/3} / r_c$, where ρ_c is the charge density in the clusters. Assuming that the charge density depends on volume fraction via $\rho_c \propto \phi_c^{-1/2}$.⁶ Using the measured charge per particle of 25 unit charges at $\phi_c = 0.006$ and $\rho_c(\phi_c^{-1/2} = 0) = 0$, we deduce $\rho_c \approx 10^{-8} \text{ nm}^{-3}$, at $\phi_c = 0.06$, which we use in the calculation.

The result of our calculation (Fig. 2a) shows that $\Delta G/N$ has a minimum at a finite size, the equilibrium size N_{eq} , which

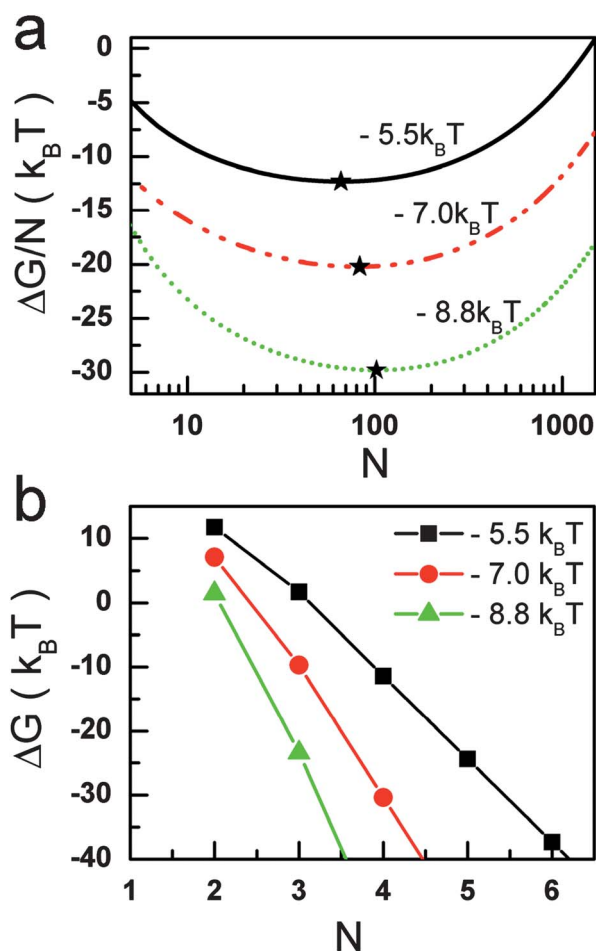


Fig. 2 $\Delta G/N$ has a minimum (marked by stars) at a finite size which increases with the strength of attraction. (b) ΔG exhibits a barrier at $N_c = 2$ for different attraction strengths. The barrier for nucleation decreases significantly with increasing the strength of short-range attractions.

increases with attraction strength, being consistent with previous studies.^{6,8} In principle, a nucleation barrier located at the critical cluster size must be overcome in order to reach the equilibrium size.⁸ To calculate the nucleation barrier the surface energy γA_c in eqn (1) is revised as $c(N)|U|N^{2/3}$ with $c(N) = 3 + 6/N$ for $N \geq 3$ and $c(N) = 5.5$ for $N = 2$. This revision is based on the maximum number of missing bonds being $6N$, *i.e.*, 12 binding sites to be shared with another particle. The number of missing bonds in a cluster is then $6N - (3N - 6) = 3N + 6$, and thus per spherical particle we have $3 + 6/N$. It can easily be verified that this correction holds for $N > 2$. For $N = 2$, we have 1 bond shared between two particles, hence $11/2 = 5.5$ missing bonds per particle. This correction is required as we will show shortly that the critical size of the clusters is usually small (<10). Clearly at large N the surface tension becomes size-independent. With this revision, Fig. 2b shows that $\Delta G(N)$ exhibits a finite barrier ΔG^* ($>1 k_B T$) for nucleation at $N_c = 2$ when the attraction strength is below $10 k_B T$. As to be expected, the nucleation barrier is smaller in systems with stronger attraction, implying a higher nucleation rate J . According to CNT, $J \propto \exp(-\Delta G^*/k_B T)$. It follows that in our systems, the nucleation rate in systems $U = -8.8 k_B T$ is about 2×10^4 times higher than that in systems with

$U = -5.5 k_B T$. This is consistent with our observation represented by Fig. 1a, d and g: the number density of stable clusters increases significantly with increasing attraction strength. Moreover, upon increasing the attraction strength, it can be seen in Fig. 1 that the concentration of single colloids ϕ_{coex} decreases. That will make it increasingly harder for the clusters to grow. Both effects of increasing attraction strength, that is, higher nucleation rate and smaller critical cluster concentration (implying smaller exchange rates of monomers between the clusters), tend to lead to smaller clusters. This is clearly a non-equilibrium effect and opposite to the trend in Fig. 2a. At this point we mention that in our calculation, when the attraction strength is stronger than $5.0 k_B T$, the critical size corresponding to the nucleation barrier is always located at $N_c = 2$ (Fig. 2b). This implies that CNT is not a good model in quantitatively predicting the value of nucleation barrier in our systems. However, we expect that the predicted trend still holds.

We now discuss the change in cluster shape upon increasing the attraction strength. In the presence of long-range repulsions, linear structures formed by one-dimensional growth have been observed before.^{4,5,12,13} Spherical clusters are possible only when the attractions are dominant.⁴ In equilibrium conditions, the long-range repulsions between particles in our systems with varying attraction strength are expected to be comparable. It follows that in our experiments, clusters should become more compact increasingly in systems with stronger attractions if they are in equilibrium. Yet, we observe quasi-linear structures in systems with the strongest attraction, *i.e.*, $U = -8.8 k_B T$ (Fig. 1e) and $U = -16.5 k_B T$ (Fig. 1h). Clusters are significantly more compact in systems with weaker attractions as shown in Fig. 1. This is again the opposite trend as observed, by computer simulation, in equilibrium clusters.⁴ Again we explain our observations by using dynamics: while compact clusters are expected to be thermodynamically more stable than linear

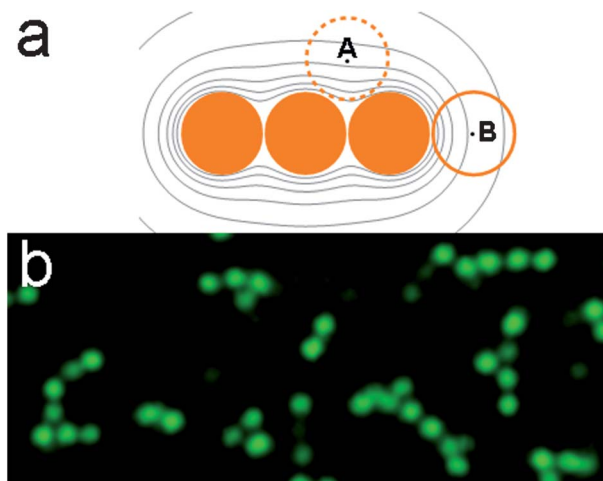


Fig. 3 (a) In the presence of long-range repulsions between particles, the kinetic barrier at position A is about 2 times of that at position B. Therefore, a linear growth is kinetically preferred because it is easier for the incoming particles to reach position B. The thin lines are the contour lines of screened coulomb potential. (b) When the rearrangement becomes a rare event at strong attractions, string-like structures are obtained at $U = -20.1 k_B T$ and $\phi_c \approx 0.07$.

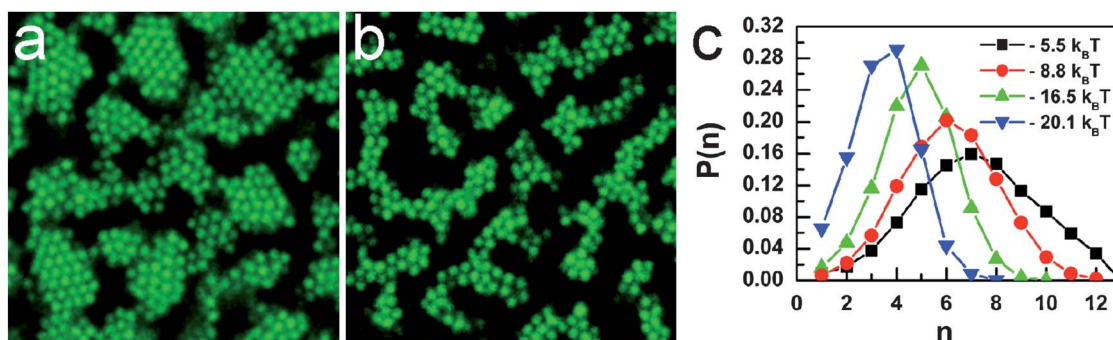


Fig. 4 Structure of gel. (a) $U = -5.5 k_B T$, $\phi_c \approx 0.36$. (b) $U = -8.8 k_B T$, $\phi_c \approx 0.20$. (c) Distribution of nearest neighbours in gels obtained at different attraction strengths.

structures under conditions studied here, due to the long-range repulsions, it is favorable for incoming particles to approach a growing cluster along a specific direction. In Fig. 3a, in the form of screened coulomb potential $\exp(-\kappa r)/r$ and $\kappa^{-1} \approx 1.6 \mu\text{m}$, it is found that the kinetic barrier for incoming particles to reach position A is about 2 times of that to reach position B. This initially gives rise to string-like structures. Subsequently, particle positions will have to rearrange to form compact clusters.

The rearrangement process will slow down upon increasing attraction strength. As a measure for the rearrangement frequency, we take the hopping rate Γ of surface particles. In its simplest (Arrhenius) form it is given by $\Gamma \approx \exp(mU)$, where m is the number of nearest neighbours of a particle located at the surface. It follows that rearrangements occur dramatically (that is, exponentially) less frequently when the short-range attractions become stronger. If the attraction is strong enough and the rearrangement becomes a rare event in experiments, string-like structures as illustrated in Fig. 3a should be obtained. To verify this trend, solutions with a very strong attraction strength of $U = -20.1 k_B T$ are prepared. In these systems, rearrangements should virtually be absent within an experimental time window. Indeed, as can be judged from Fig. 3b, string-like clusters are obtained at $\phi_c \approx 0.07$. Rearrangements of the string-like structures have not been observed on the experimental time scale. The formation of string-like structures is fundamentally different from the classical ‘‘Diffusion Limited Cluster Aggregation’’ and ‘‘Reaction Limited Cluster Aggregation’’ in that effectively, electrostatic interactions cause directionality.

Except giving rise to the kinetic barriers as exemplified by Fig. 3a, the long range Coulomb interactions also play a role in preventing the further coarsening of microcrystallites and further coarsening by collision of colloidal clusters in the non-equilibrium cluster phases as shown in Fig. 1d and g. In previous studies, it has been found that the cluster phases can also be in a non-ergodic state: a Wigner glass of clusters^{13,15,24} in which clusters are caged by the long-range repulsions between them. To test that would require the mean square displacement of the clusters over (very) long times. In the systems studied here, on these long time scales, sedimentation of the clusters becomes important so at this point we are unable to conclude whether the clusters are in a dynamically arrested state.

Upon increasing the volume fraction, eventually gels are formed. However, the routes to gel are different in systems with different attraction strengths. In solutions with $U = -5.5 k_B T$, as Fig. 1a–c illustrate, upon increasing the local volume fraction, more and more crystalline clusters are formed and finally, the system gets arrested by crowding, giving rise to microcrystalline gels (Fig. 4a).²¹ This scenario is similar to the mechanism of jamming suggested by Segrè *et al.*¹⁴ However, in solutions with $U = -8.8 k_B T$ (Fig. 1d–f) and $U = -16.5 k_B T$ (Fig. 1g–i), clusters become elongated and branched. These percolating clusters finally get interconnected through the whole systems (Fig. 4b). This scenario of gelation is similar to the mechanism of percolation as observed by Toledano *et al.*¹³ The bond number distribution in gels (Fig. 4c) shows that upon increasing strength of attractions, the peak of the distribution shifts to smaller number, suggesting that the local structures become thinner due to the stronger attractions. In that respect, the morphology of the gel reflects the shape of the clusters from which it has been evolved.

Moreover, in previous studies,^{25,26} ordered modulated structures were observed by simulation in small systems and it was suggested that gels in systems with competing short-range attractions and long-range repulsions are generally a consequence of arrested microphase separations. However, the ordered modulated structures have never been observed in experiments. A possible mechanism, as can be seen in Fig. 4a and b, is that the polydispersity and the irregular shape of clusters hinder the evolution from a gel structure to an ordered modulated structure. In previous studies,¹⁰ slow aging of the gels has been observed. While slow aging might also occur in the clusters, similar to aging of the gel state, we have been unable to detect that with our setup.

Conclusion

In summary, we find that in colloidal systems with competing short-range attractions and long-range repulsions, non-equilibrium effects play a key role and should be taken into account. The strength of the short-range attractions determines the mechanism of nucleation and growth, and thereby the size, shape, and structure of the clusters. The properties of the clusters, in turn, determine the mechanism of gelation and the

structure of the gels being formed at relatively high volume fractions.

Acknowledgements

We thank Dr Els de Hoog from NIZO Food Research for helping with confocal microscope and data collection. We acknowledge the financial support by Netherlands Institute for Space Research (SRON).

Notes and references

- 1 V. J. Anderson and H. N. W. Lekkerkerker, *Nature*, 2002, **416**, 811.
- 2 P. N. Pusey, A. D. Pirie and W. C. K. Poon, *Phys. A*, 1993, **201**, 322.
- 3 E. H. A. de Hoog, W. K. Kegel, A. van Blaaderen and H. N. W. Lekkerkerker, *Phys. Rev. E: Stat. Phys., Plasmas, Fluids, Relat. Interdiscip. Top.*, 2001, **64**, 021407.
- 4 S. Mossa, F. Sciortino, P. Tartaglia and E. Zaccarelli, *Langmuir*, 2004, **20**, 10756.
- 5 F. Sciortino, P. Tartaglia and E. Zaccarelli, *J. Phys. Chem. B*, 2005, **109**, 21942.
- 6 J. Groenewold and W. K. Kegel, *J. Phys. Chem. B*, 2001, **105**, 11702.
- 7 H. Sedgwick, S. U. Egelhaaf and W. C. K. Poon, *J. Phys.: Condens. Matter*, 2004, **16**, S4913.
- 8 S. B. Hutchens and Z.-G. Wang, *J. Chem. Phys.*, 2007, **127**, 084912.
- 9 A. Stradner, H. Sedgwick, F. Cardinaux, W. C. K. Poon, S. U. Egelhaaf and P. Schurtenberger, *Nature*, 2004, **432**, 492.
- 10 M. M. van Schooneveld, V. W. A. de Villeneuve, R. P. A. Dullens, D. G. A. L. Aarts, M. E. Leunissen and W. K. Kegel, *J. Phys. Chem. B*, 2009, **113**, 4560.
- 11 R. Sanchez and P. Bartlett, *J. Phys.: Condens. Matter*, 2005, **17**, S3551.
- 12 A. I. Campbell, V. J. Anderson, J. S. van Duijneveldt and P. Bartlett, *Phys. Rev. Lett.*, 2005, **94**, 208301.
- 13 J. C. F. Toledano, F. Sciortino and E. Zaccarelli, *Soft Matter*, 2009, **5**, 2390.
- 14 P. N. Segrè, V. Prasad, A. B. Schofield and D. A. Weitz, *Phys. Rev. Lett.*, 2001, **86**, 6042.
- 15 F. Sciortino, S. Mossa, E. Zaccarelli and P. Tartaglia, *Phys. Rev. Lett.*, 2004, **93**, 055701.
- 16 R. P. A. Dullens, M. Claesson, D. Derks, A. van Blaaderen and W. K. Kegel, *Langmuir*, 2003, **19**, 5963.
- 17 H. N. W. Lekkerkerker, W. C. K. Poon, P. N. Pusey, A. Stroobants and P. B. Warren, *Europhys. Lett.*, 1992, **20**, 559.
- 18 S. Asakura and F. Oosawa, *J. Polym. Sci., Polym. Symp.*, 1958, **33**, 183.
- 19 M. E. Leunissen, A. van Blaaderen, A. D. Hollingsworth, M. T. Sullivan and P. M. Chaikin, *Proc. Natl. Acad. Sci. U. S. A.*, 2007, **104**, 2585.
- 20 J. C. Crocker and D. G. Grier, *J. Colloid Interface Sci.*, 1996, **179**, 298.
- 21 T. H. Zhang, J. Groenewold and W. K. Kegel, *Phys. Chem. Chem. Phys.*, 2009, **11**, 10827.
- 22 J. N. Israelachvili, *Intermolecular and Surface Forces*, Academic Press, London, 1992.
- 23 H. Reiss, W. K. Kegel and J. Groenewold, *Ber. Bunsen-Ges. Phys. Chem.*, 1996, **100**, 279.
- 24 C. L. Klix, C. P. Royall and H. Tanaka, *Phys. Rev. Lett.*, 2010, **104**, 165702.
- 25 P. Charbonneau and D. R. Reichman, *Phys. Rev. E: Stat., Nonlinear, Soft Matter Phys.*, 2007, **75**, 050401(R).
- 26 A. d. Candia, E. D. Gado, A. Fierro, N. Sator, M. Tarzia and A. Coniglio, *Phys. Rev. E: Stat., Nonlinear, Soft Matter Phys.*, 2006, **74**, 010403(R).